In vivo movement of the type V myosin Myo52 requires dimerisation but is independent of the neck domain

Agnes Grallert[1], Rebeca Martín-García[2], Steve Bagley[3] and Daniel P. Mulvihill[2,*]

[1]Cancer Research UK Cell Division Group, CR-UK Paterson Institute for Cancer Research, Manchester, M20 4BX, UK
[2]Cell and Developmental Biology Group, Department of Biosciences, University of Kent, Canterbury, Kent, CT2 7NJ, UK
[3]Advanced imaging facility, CR-UK Paterson Institute for Cancer Research, Manchester, M20 4BX, UK
*Author for correspondence (e-mail: d.p.mulvihill@kent.ac.uk)

Accepted 10 September 2007
Journal of Cell Science 120, 4093-4098 Published by The Company of Biologists 2007
doi:10.1242/jcs.012468

Summary

Intracellular movement is a fundamental property of all cell types. Many organelles and molecules are actively transported throughout the cytoplasm by molecular motors, such as the dimeric type V myosins. These possess a long neck, which contains an IQ motif, that allow it to make 36-nm steps along the actin polymer. Live cell imaging of the fission yeast type V myosin Myo52 reveals that the protein moves rapidly throughout the cytoplasm. Here, we describe analysis of this movement and have established that Myo52 moves long distances on actin filaments in an ATP-dependent manner at ~0.5 μm/second. Myo51 and the microtubule cytoskeleton have no discernable role in modulating Myo52 movements, whereas rigour mutations in Myo52 abrogated its movement. We go on to show that, although dimerisation is required for Myo52 movement, deleting its neck has no discernable affect on Myo52 function or velocity in vivo.

Supplementary material available online at
http://jcs.biologists.org/cgi/content/full/120/23/4093/DC1

Key words: *Schizosaccharomyces pombe*, Myosin V, IQ domains

Introduction

Myosin V proteins are dimeric-actin-associated motor proteins involved in diverse cell biological processes (Mehta et al., 1999). They possess four distinct domains: the motor domain, the neck region that normally contains six IQ motifs to which light chains bind, the coiled-coil region to facilitate dimerisation and the globular tail to which cargoes bind. Although type V myosins have been characterised biochemically, the regions within the motor domain that give it its distinctive motor activity are not yet well understood. Recent studies have brought into question fundamental properties of myosin Vs, including the role played by the neck region in determining the step-size of myosin Vs when 'walking' along actin cables. Step size is normally 36 nm, which coincides with the helical repeat of actin (Mehta et al., 1999). Research using myosin V head constructs (lacking neck and tail domains) has suggested that step size is independent of the presence of IQ domains (Tanaka et al., 2002; Watanabe et al., 2004). This is in contrast to studies using full-length myosin V, which indicate a direct relationship between neck-length, step size and sliding-filament velocities, with myosin V possessing six IQs moving significantly faster (0.36±0.08 μm/second) than a myosin V with a shorter, two IQ-motif-containing neck (0.29±0.07 μm/second) (Purcell et al., 2002; Sakamoto et al., 2003; Sakamoto et al., 2005; Schott et al., 2002). In addition, it is also unclear at present whether myosin Vs have a conserved motor function between organisms, because studies to date suggest the budding yeast and *Drosophila* myosin Vs move non-processively along actin (Reck-Peterson et al., 2001; Toth et al., 2005).

Myo51 and Myo52 are the fission yeast type myosin Vs, each with distinctive functions. Myo51 primarily functions during the meiotic lifecycle (A. Doyle, R.M.-G., S.B. and D.P.M., unpublished), whereas Myo52 has multiple functions during the vegetative cycle. Myo51 localises to the actin ring during the mitotic cell cycle, whereas Myo52 localises to foci that move throughout the cytoplasm, concentrating at regions of cell growth (Motegi et al., 2001; Win et al., 2001). Here, we characterise Myo52 movements and movements of novel Myo52 mutants – including rigour mutants; of a Myo52 mutant that lacks its coiled-coil domain and is therefore unable to dimerise; and of a mutant lacking its entire neck domain. The latter moved and functioned normally within the cell, indicating the neck domain is not required for myosin V motor function in vivo, and that properties other than the neck size determines the cellular velocity of the protein.

Results and Discussion

Myo52 in vivo movements

The fission yeast, *Schizosaccharomyces pombe*, is amenable to live cell imaging techniques allowing in vivo analysis of movements of one of its class V myosin, Myo52. Using strains in which the chromosomal copy of the *myo52* gene had been fused to cDNA encoding GFP at either the N-terminal (Myo52-nGFP) or the C-terminal (Myo52-cGFP) end, we analysed over 1000 individual in vivo movements (supplementary material Movie 1) of Myo52, which revealed at least two distinct types

of Myo52 movement. One was a brief, slow (~0.25 μm/second) and erratic movement with Myo52 moving a short distance before either stopping or moving in a different direction (focal movement had no discrete direction over three subsequent time points, with movements seeming random; Fig. 1a, yellow and green arrows). The other was of a higher velocity and with an easily discernable overall direction towards either a cell pole or the cell equator, with foci moving on a discernable path for at least three subsequent frames (often up to 20 frames; Fig. 1a, red, white and blue arrowheads). Kymograph analyses highlight the distinctions between the rapid and slow classes of movement (Fig. 1g). The position of the GFP fluorophore on Myo52 did not affect the velocity or duration of movements (Myo52-nGFP: 0.502±0.09 μm/second; Myo52-cGFP: 0.511±0.07 μm/second). We observed no bias in rapid Myo52 movements towards any particular cellular locus, or any significant differences in the velocity of cytoplasmic Myo52 movements (e.g. any correlation to the cell cycle, differential brightness of Myo52 foci, Myo52 expression levels or cellular location). Bi-directional movements were often seen (Fig. 1a, white arrow; Fig. 1g,h, asterisks), probably brought about by the complex actin filament network in *S. pombe*.

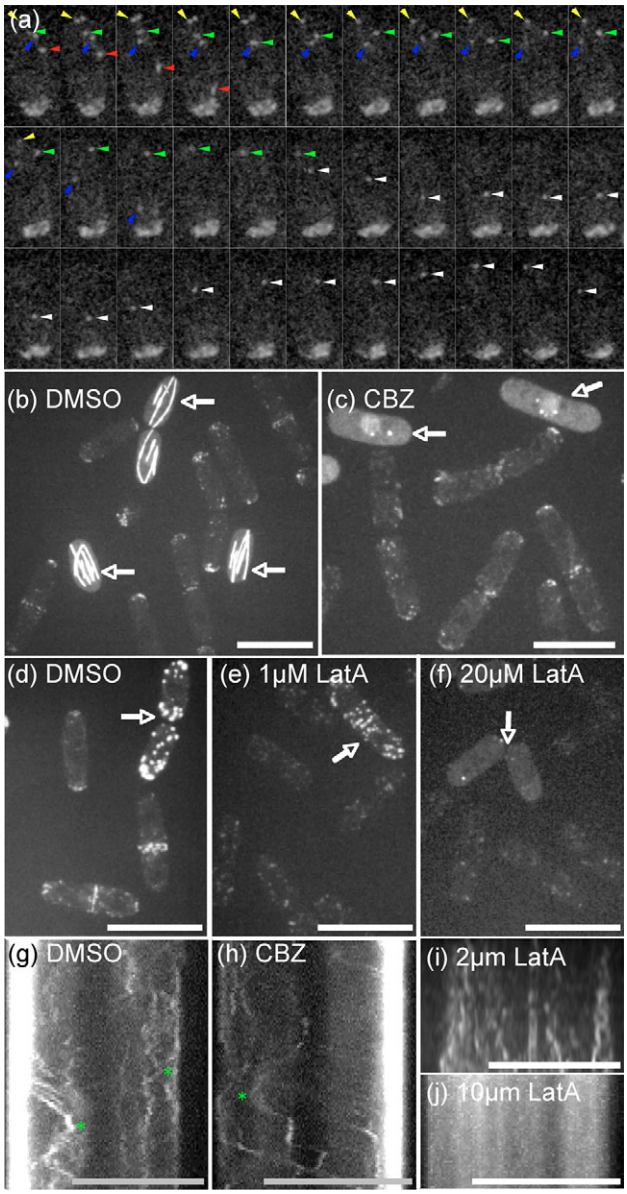

Fig. 1. In vivo analysis of Myo52 movement. (a) Live timelapse analysis of the Myo52-cGFP strain revealed slow short movements (yellow and green arrows) and fast long directed movements (red, white and blue arrows). Myo52 foci are often seen to change poleward direction of travel (white arrow). (b,c) Cells expressing either Myo52-nGFP or GFP-Atb2 (arrows) were mixed and Myo52 movements were monitored in the (b) absence or (c) presence of 25 μg/ml carbendazim. Microtubule depolymerisation did not affect Myo52 movement. (d-f) Myo52 movements and the actin-patch movement were monitored simultaneously in cells expressing either Myo52-nGFP or Crn1-GFP (arrows) when they were incubated in the presence of (d) DMSO, (e) 2 μM or (f) 20 μM latrunculin A. (g-j) Kymographs of 100×100 msecond timelapse frames of Myo52-cGFP cells treated with (g) DMSO, (h) carbendazim, (i) 2 μM or (j) 20 μM latrunculin A demonstrate that rapid long-distance Myo52 movements are not affected by microtubule depolymerisation but abolished in the absence of actin cables. Bars, 10 μm.

Myo52 movement and microtubules

Studies from diverse organisms show a functional relationship between Myosin V proteins and microtubules (Cao et al., 2004; Huang et al., 1999; Motegi et al., 2001; Wu et al., 2005). To determine whether rapid long-distance mobility of Myo52 relies upon the movement of kinesin on microtubules, its movements were monitored in cells treated with the microtubule-depolymerizing drug carbendazim. Addition of 25 μg/ml carbendazim led to a rapid disappearance of microtubules, seen in nmt81*gfp-atb2* cells (Fig. 1c, arrows). Microtubule depolymerisation had no affect upon Myo52 movement or its ability to switch direction (Fig. 1h; supplementary material Movies 2 and 3). Furthermore Myo52 movement was not affected in strains that lack kinesins with overlapping function – such as the two Kar3-like kinesins (*pkl1Δklp2Δ* cells) – or both central-motor-centromere-associated kinesins (*klp5Δ klp6Δ* cells), and in strains lacking any single kinesin alone. Consistent with these findings Myo52 foci were never seen associated with microtubules when visualised simultaneously in the same cells (supplementary material Fig. S1a). Simultaneous observation of Myo52 and microtubules in this *HcRed1-myo52 gfp-atb2* strain also allowed us to follow recruitment of Myo52 to the cell equator during the metaphase-anaphase transition, when microtubules are incorporated into the short (2.1±0.4 μm) mitotic spindle at the cell equator. Myo52 then moves from the cell tips, extending 6.4±0.3 μm from the cell equator, which indicates that microtubules cannot be involved in the medial recruitment of Myo52. Inhibition of this medial recruitment by microtubule depolymerisation (Motegi et al., 2001) is therefore likely to be due to the action of either a checkpoint mechanism or regulating molecules recruited to the cell equator by microtubules.

Myo52 movement is dependent upon actin filaments

We went on to establish whether Myo52 movement is dependent upon actin. When compared with cortical actin patches, actin filaments have a higher susceptibility to the F-actin depolymerising affects of the drug latrunculin A and

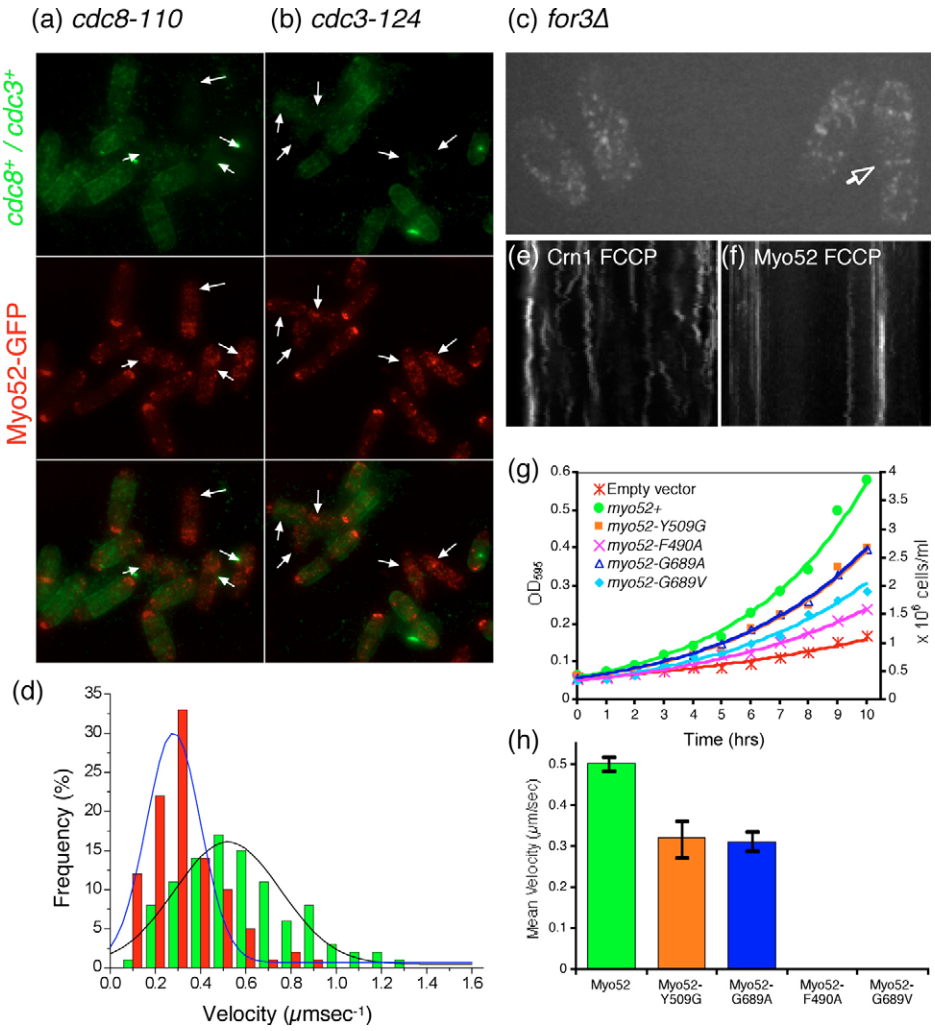

Fig. 2. Myo52 movement upon actin filaments is driven by its own motor activity drives. (a,b) Myo52-cGFP localisation (middle panels, red labelling in bottom panels) is abolished in mutant cells (arrows) that lack (a) the fission yeast tropomyosin or (b) profillin, but not in simultaneously observed TRITC-lectin-labelled wild-type cells (upper panels, green labelling in bottom panels). (c) Myo52 links with medial-ring-associated actin filaments in *for3Δ* cells, lacking the normal interphase filament distribution. (d) Velocity distributions of Myo52 foci (green) and GFP-Crn1 labelled actin patches (red) are significantly different. (e,f) ATP depletion using 10 nM FCCP abolishes (f) Myo52 but not (e) actin-patch movement. (g) Point mutations introduced to residues within the Myo52 protein that were predicted to disrupt the motor function of the protein. Growth curves indicate that none of the mutant proteins were able to complement the *myo52Δ* allele. (h) Compared with wild-type Myo52 movements of these rigour mutants had a reduced velocity (Y509G and G689A) or were abolished completely (F490A and G689V).

allows the opportunity to examine Myo52 in the absence of specific components of the actin cytoskeleton. Actin structures can be monitored simultaneously by following movements of the actin patch component Crn1 (Pelham and Chang, 2001) (supplementary material Movie 4). Treatment with 1 μM latrunculin depolymerised actin filaments as determined by actin patches losing their polarised localisation pattern and ceasing to move (Fig. 1e, white arrow). Latrunculin also abolished rapid long-distance Myo52 movements (Fig. 1i; supplementary material Movie 5) but did not affect slow short-range movements. The addition of 20 μM latrunculin resulted in the depolymerisation of all F-actin structures, as observed by the loss of a discrete GFP-Crn1 signal (Fig. 1f – white arrow). Similarly, all measurable Myo52 movements were abolished and foci disappeared within a few minutes (Fig. 1f; supplementary material Movie 6).

We investigated the role of different actin-containing structures in Myo52 movements by using conditional mutants. Inactivation of the *S. pombe* tropomyosin homologue Cdc8 destabilises actin filaments, whereas inactivation of profillin (Cdc3) renders cells incapable of forming F-actin structures (Balasubramanian et al., 1992; Balasubramanian et al., 1994). These conditional mutants confirmed our findings in that long distance movements were abolished in *cdc8-110* (Fig. 2a) and *cdc3-124* (Fig. 2b) cells at the restrictive temperature. In addition, Myo52 was only seen to move at the cell equator in cells that lack the formin For3 and that only possess CAR-associated actin filaments (Fig. 2c, supplementary material Movie 7) (Feierbach and Chang, 2001). Together, these data indicate that Myo52 moves upon actin filaments to yielding rapid long-distance movements.

Myo52 moves actively upon actin filaments

Having established that rapid Myo52 movements are dependent upon the presence of actin cables, we asked whether Myo52 movement arises from an attachment to polymerizing and depolymerising actin cables, and therefore represents a passive mode of transport. We compared velocities of the actin patch component Crn1, which gives a direct readout of actin-cable dynamics, with those of directional Myo52 movement. The velocity of 1375 Myo52-foci movements fitted a Gaussian distribution with an average velocity of 0.51 μm/second (Fig. 2d), with no significant difference between the distribution of Myo52 movements to poles or equator. As Myo52 velocity does not change at different positions within the cell, it suggests that mechanisms regulating Myo52-driven movement operate uniformly throughout the cell. A population of 247 individual, directed Crn1 foci movements fitted a narrow Gaussian distribution, with a mean velocity of 0.28±0.04 μm/second. Student's *t*-test analysis indicated that the two

Table 1. Summary of cellular velocities

Protein	Challenge	Comments	Velocity* (μm/second)	*n*
GFP-Myo52	None	N-terminally GFP-tagged Myo52 expressed from chromosome in *myo52Δ* background	0.502±0.09	403
GFP-Myo52	None	N-terminally GFP-tagged Myo52 expressed from multicopy plasmid in *myo52Δ* background	0.508±0.07	362
Myo52-GFP	None	C-terminally GFP-tagged Myo52 expressed from endogenous locus	0.511±0.06	972
Myo52-GFP	*myo51Δ* strain	Gene encoding Myo51, a second myosin V, deleted from *S. pombe* genome	0.518±0.08	216
GFP-Crn1	None	Actin-patch marker	0.28±0.04	147
Myo52-GFP	Nitrogen-starved cells	Disorganised actin cytoskeleton	0	–
Myo52-GFP	Glucose-starved cells	Cells subjected to nutrient stress	No effect	–
Myo52-GFP	Cells in sorbitol (1.2 M)	Cells subjected to osmotic stress	No effect	–
Myo52-GFP	CBZ (25 μg/ml)	No microtubules	0.507±0.07	132
Myo52-GFP	Latruncullin A (1 μM)	No actin filaments	0	–
Myo52-GFP	Latruncullin A (20 μM)	No actin structures	0	–
Myo52-GFP	*cdc3-124* strain at 36°C	No F-actin	0	–
Myo52-GFP	*cdc8-110* strain at 36°C	No actin filaments	0	–
Myo52-GFP	*for3Δ* strain	No interphase actin filaments	0	–
GFP-Crn1	FCCP (10 nM)	Reduced cellular [ATP]	0.265±0.04	104
Myo52-GFP	FCCP (10 nM)	Reduced cellular [ATP]	0	–
GFP-Myo52ΔIQ	None	Myo52 lacking neck region in *myo52Δ* background	0.522±0.14	233

*Directed cytoplasmic movements only.

populations differ significantly (99.99% confidence), and show that Myo52 moves almost twice as fast as actin filaments grow and shrink, indicating it is not moving passively on growing actin polymers.

As Myo52 movement is unaffected by the absence of Myo51 (Table 1), its movement is likely to be a result of its own ATPase activity and should, therefore, be dependent upon ATP. To investigate this further, cells were treated with the oxidative-phosphorylation uncoupler carbonyl cyanide p-trifluoromethoxyphenyl-hydrazone (FCCP), to rapidly reduce levels of cellular ATP (Cheng et al., 2003). At concentrations of FCCP that reduced ATP levels more than 1000 times (determined by luciferase assay), Myo52 foci ceased to move throughout the cytoplasm (Fig. 2f), indicating that the movement of Myo52 upon actin filaments is an active process.

Introducing mutations within Myo52 can be used to modulate its interaction with actin, which in turn might affect its cellular velocity. Mutating residues within the conserved relay loop responsible for communicating movements between the active site and the actin-binding site (Tsiavaliaris et al., 2002) or mutating the conserved glycine residue within the reactive thiol region (Batra et al., 1999;

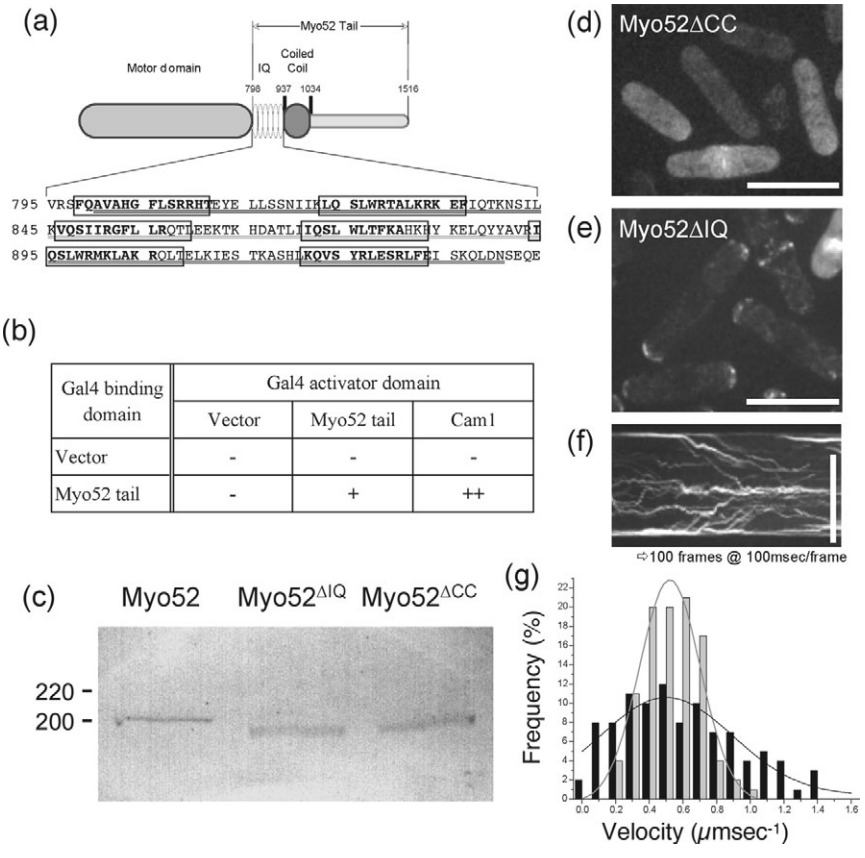

Fig. 3. Myo52 function and movement are not dependent upon its neck region. (a) Myo52 protein with boxed IQ-motif sequences. Residues deleted from GFP-Myo52ΔIQ are underlined. (b) Yeast two-hybrid assay showing interaction of the Myo52 tail with itself or the fission yeast calmodulin Cam1. (c) Anti-GFP western blot of *myo52Δ*-strain extracts expressing Myo52-nGFP, GFP-Myo52ΔIQ or GFP-Myo52ΔCC confirm the expected reduced size of the Myo52 mutant in the latter strain. (d,e) Micrographs of (d) Myo52ΔCC and (e) Myo52ΔIQ cells show that only Myo52ΔIQ localised normally and was able to complement the morphology defect associated with the *myo52Δ* allele. (f) Kymographs of Myo52ΔIQ cells demonstrate that the truncation mutant can make rapid directed and bidirectional movements throughout the cell. (g) Velocity distributions of Myo52 and Myo52ΔIQ. Bars, 10 μm.

Uyeda et al., 2002) can change the affinity of myosin for actin. We therefore created strains that constitutively express Myo52-nGFP and contain comparable mutations within its motor domain. None of these mutants fully complemented the *myo52Δ* phenotype, and resulted in either a reduction in Myo52 velocity (Y509G & G689A) or abolition of Myo52 movements (F490A and G689V) (Fig. 2g,h). These data demonstrate that the movement of Myo52 foci is the result of their own Myo52 motor activity, which is necessary for Myo52 function in the cell.

Movement and velocity of Myo52 are not dependent upon the neck region

Having established that Myo52 moves actively on actin cables, we made use of this in vivo assay to examine the role individual domains play in facilitating its movement (Fig. 3a). Using the yeast two-hybrid assay, we examined whether (1) the short coiled-coil domain of Myo52 (107 residues) can dimerise – because this domain is significantly longer in myosin V proteins of *Drosophila* and vertebrates (500 residues) and, (2) whether Myo52 associates with calmodulin, a conserved IQ-motif-binding protein. The ability of the Myo52 tail (neck, coiled-coil and globular-tail domain; Fig. 3a) to interact with itself suggests that Myo52 can indeed dimerise. Its high affinity to the fission yeast calmodulin Cam1 suggests that calmodulin can bind to Myo52 (Fig. 3b).

Constructs that express Myo52-nGFP but lack the entire Myo52 neck region (GFP-Myo52ΔIQ, lacking residues 800-940) or the coiled-coil domain (GFP-Myo52ΔCC, lacking residues 940-1060) were created and integrated into the genome of *myo52Δ* cells. Both truncations resulted in the expected increase of mobility in SDS-PAGE experiments (Fig. 3c). Myo52ΔCC was seen to localise only weakly to the cell equator and only partially complemented the growth defects associated with *myo52Δ* cells (Fig. 3d). It never localised to motile foci within the cell, indicating that dimerisation is required for Myo52 function and in vivo movement. By contrast, the cellular distribution of Myo52ΔIQ was indistinguishable from that of the full-length protein (Fig. 3e). Kymographs of timelapse movies of GFP-Myo52ΔIQ cells demonstrated that the protein was capable of making slow, rapid, and bidirectional movements (Fig. 3f, supplementary material Movie 8). The Myo52ΔIQ truncation was able to complement the growth and morphology defects associated with *myo52Δ* cells (Fig. 3e). Myo52ΔIQ did not associate with the IQ-motif-binding calmodulin light chains and is unlikely to be able to make the predicted 36-nm steps along the actin helix repeat. However, these data demonstrate that deleting all six IQ domains has no effect on in vivo movement of Myo52 and suggest the neck region is not required for it to function within the cell. Analysis of 233 rapid, directed movements of Myo52ΔIQ revealed that the velocities (mean velocity 0.522±0.14 μm/second) fitted a tight Gaussian curve (Fig. 3g). The mean velocity of Myo52ΔIQ does not differ significantly from that obtained for the full-length protein (0.502±0.09 μm/second), which suggests that deletion of the IQ motifs does not have an adverse affect on the motor properties of the protein. The ability of Myo52 to dispense with its neck for normal in vivo function highlights differences in the evolutionary and functional significance IQ motifs of the neck regions play in myosin V proteins of different organisms; moreover, this phenomenon has not been found in any vertebrate myosin V described to date, showing that the cellular velocity of Myo52 is determined by properties other than neck length. Multiple Myo52 dimers may associate into arrays capable of working together with coiled-coils acting as lever arms, indicating that Myo52 might be capable of functioning non-processively under these conditions. It is unlikely that the coiled-coil region of Myo52 replaces the IQ neck region as a lever arm in Myo52ΔIQ, because its shorter length (97 residues compared with 139 residues) would result in the protein having a reduced cellular velocity. In addition, the lever would be unable to operate in a processive manner, because there would be only one lever for two heads. Similarly, the short length of the coiled-coil domain indicates that the region is not used as a flexible linker – like the coiled-coil within myosin VI – to allow stretching between actin sites. Even if the coiled-coil domain were able to unwind completely it would not be capable of reaching the same distance as the neck.

Although removal of the IQ domains had no effect on the mean velocity of Myo52, the distribution of Myo52 and Myo52ΔIQ foci velocities differ significantly, and indicate that the IQ domain might regulate Myo52 function – potentially through binding to light chains or by allowing the globular tail domain to associate with the motor domains, thus inhibiting motor function (Liu et al., 2006; Thirumurugan et al., 2006).

Materials and Methods

Yeast cell culture and strains

The strains used in this study are listed in supplementary material Table S1. Cell culture and maintenance were carried out as describen previously (Moreno et al., 1991). Cells were grown in filter-sterilized minimal (EMM2) supplemented media.

Western blotting

5×10^7 cells were harvested from mid-log phase cultures of *S. pombe* cells, washed in ice-cold STOP buffer (Moreno et al., 1991; Simanis and Nurse, 1986), and frozen in liquid nitrogen prior to storage at –80°C. Protein was extracted by resuspending cells in EXPY buffer [HE buffer (Simanis and Nurse, 1986) supplemented with 1 μg/ml AEBSF, 1 μg/ml antipain, 1 μg/ml aprotinin, 10 μM benzamidine, 1 μg/ml chymostatin, 1 μg/ml E64, 1 μg/ml leupeptin, 1 μg/ml pepstatin, 5 μM phenanthroline, and 1 mM PMSF] and disrupting them with 500 μl of acid-washed glass beads in a ThermoSavant Fastprep 120 (MP Biochemicals, Irvine, USA). Samples were then boiled with SDS-PAGE loading buffer. Western blotting detection was carried out using alkaline phosphatase reagents. Anti-GFP antibodies (generous gift from W. Gullick, University of Kent) were used at a 1:100 dilution.

Fluorescence microscopy

Live cells were grown, visualised and images were processed as described previously (Grallert et al., 2006). Cells were visualised on a Deltavision Spectris system (Applied Precision Instruments), based around an Olympus IX71 microscope. Enclosed in an opaque environmental chamber, the system uses a Zeiss Alpha-Plan-Fluar ×100 1.45NA objective lens and a Sedat ET-filter set (Chroma) which is located on external filter wheels. Illumination is via a Sutter 300W xenon light source, which is delivered to the microscope through a liquid light guide. All of the equipment is isolated through an anti-vibration table and all components that create vibration are isolated from the microscope. The hardware is controlled by a Win95 PC, whereas the capture software is on a Linux Redhat PC; the software used to control image capture is softworx (API).

Object tracking

Cells were cultured and imaged in minimal media at 25°C (unless stated otherwise) as described above. Once the type of movement had been determined (by following its movement using a maximum projection timelapse of the *z* series stacks), the time elapsed and distance moved (3D) between the frames and the moved dot were determined manually using Imaris image analysis or Metamorph particle-tracking software (Molecular Devices, Downington, PA). The tracking continued until either no detectable movement was observed or until the dot moved out of the field of view. This was repeated for several 100, independent Myo52 movements and used to describe a population distribution of Myo52 movements.

We thank P. Nurse and F. Chang for strains, and I. Hagan and M. Geeves for their support and comments on the manuscript. This work was supported by the BBSRC (a David Phillips Fellowship to D.P.M.) and Cancer Research UK (CRUK).

References

Balasubramanian, M. K., Helfman, D. M. and Hemmingsen, S. M. (1992). A new tropomyosin essential for cytokinesis in the fission yeast S. pombe. *Nature* **360**, 84-87.

Balasubramanian, M. K., Hirani, B. R., Burke, J. D. and Gould, K. L. (1994). The Schizosaccharomyces pombe cdc3+ gene encodes a profilin essential for cytokinesis. *J. Cell Biol.* **125**, 1289-1301.

Batra, R., Geeves, M. A. and Manstein, D. J. (1999). Kinetic analysis of Dictyostelium discoideum myosin motor domains with glycine-to-alanine mutations in the reactive thiol region. *Biochemistry* **38**, 6126-6134.

Cao, T. T., Chang, W., Masters, S. E. and Mooseker, M. S. (2004). Myosin-Va binds to and mechanochemically couples microtubules to actin filaments. *Mol. Biol. Cell* **15**, 151-161.

Cheng, G., Polito, C. C., Haines, J. K., Shafizadeh, S. F., Fiorini, R. N., Zhou, X., Schmidt, M. G. and Chavin, K. D. (2003). Decrease of intracellular ATP content downregulated UCP2 expression in mouse hepatocytes. *Biochem. Biophys. Res. Commun.* **308**, 573-580.

Feierbach, B. and Chang, F. (2001). Roles of the fission yeast formin for3p in cell polarity, actin cable formation and symmetric cell division. *Curr. Biol.* **11**, 1656-1665.

Grallert, A., Beuter, C., Craven, R. A., Bagley, S., Wilks, D., Fleig, U. and Hagan, I. M. (2006). S. pombe CLASP needs dynein, not EB1 or CLIP170, to induce microtubule instability and slows polymerization rates at cell tips in a dynein-dependent manner. *Genes Dev* **20**, 2421-2436.

Huang, J. D., Brady, S. T., Richards, B. W., Stenolen, D., Resau, J. H., Copeland, N. G. and Jenkins, N. A. (1999). Direct interaction of microtubule- and actin-based transport motors. *Nature* **397**, 267-270.

Liu, J., Taylor, D. W., Krementsova, E. B., Trybus, K. M. and Taylor, K. A. (2006). Three-dimensional structure of the myosin V inhibited state by cryoelectron tomography. *Nature* **442**, 208-211.

Mehta, A. D., Rock, R. S., Rief, M., Spudich, J. A., Mooseker, M. S. and Cheney, R. E. (1999). Myosin-V is a processive actin-based motor. *Nature* **400**, 590-593.

Moreno, S., Klar, A. and Nurse, P. (1991). Molecular genetic analysis of fission yeast Schizosaccharomyces pombe. *Methods Enzymol* **194**, 795-823.

Motegi, F., Arai, R. and Mabuchi, I. (2001). Identification of two type V myosins in fission yeast, one of which functions in polarized cell growth and moves rapidly in the cell. *Mol. Biol. Cell* **12**, 1367-1380.

Pelham, R. J., Jr and Chang, F. (2001). Role of actin polymerization and actin cables in actin-patch movement in Schizosaccharomyces pombe. *Nat. Cell Biol.* **3**, 235-244.

Purcell, T. J., Morris, C., Spudich, J. A. and Sweeney, H. L. (2002). Role of the lever arm in the processive stepping of myosin V. *Proc. Natl. Acad. Sci. USA* **99**, 14159-14164.

Reck-Peterson, S. L., Tyska, M. J., Novick, P. J. and Mooseker, M. S. (2001). The yeast class V myosins, Myo2p and Myo4p, are nonprocessive actin-based motors. *J. Cell Biol.* **153**, 1121-1126.

Sakamoto, T., Wang, F., Schmitz, S., Xu, Y., Xu, Q., Molloy, J. E., Veigel, C. and Sellers, J. R. (2003). Neck length and processivity of myosin V. *J. Biol. Chem.* **278**, 29201-29207.

Sakamoto, T., Yildez, A., Selvin, P. R. and Sellers, J. R. (2005). Step-size is determined by neck length in myosin V. *Biochemistry* **44**, 16203-16210.

Schott, D. H., Collins, R. N. and Bretscher, A. (2002). Secretory vesicle transport velocity in living cells depends on the myosin-V lever arm length. *J. Cell Biol.* **156**, 35-39.

Simanis, V. and Nurse, P. (1986). The cell cycle control gene cdc2+ of fission yeast encodes a protein kinase potentially regulated by phosphorylation. *Cell* **45**, 261-268.

Tanaka, H., Homma, K., Iwane, A. H., Katayama, E., Ikebe, R., Saito, J., Yanagida, T. and Ikebe, M. (2002). The motor domain determines the large step of myosin-V. *Nature* **415**, 192-195.

Thirumurugan, K., Sakamoto, T., Hammer, J. A., 3rd, Sellers, J. R. and Knight, P. J. (2006). The cargo-binding domain regulates structure and activity of myosin 5. *Nature* **442**, 212-215.

Toth, J., Kovacs, M., Wang, F., Nyitray, L. and Sellers, J. R. (2005). Myosin V from Drosophila reveals diversity of motor mechanisms within the myosin V family. *J. Biol. Chem.* **280**, 30594-30603.

Tsiavaliaris, G., Fujita-Becker, S., Batra, R., Levitsky, D. I., Kull, F. J., Geeves, M. A. and Manstein, D. J. (2002). Mutations in the relay loop region result in dominant-negative inhibition of myosin II function in Dictyostelium. *EMBO Rep.* **3**, 1099-1105.

Uyeda, T. Q., Tokuraku, K., Kaseda, K., Webb, M. R. and Patterson, B. (2002). Evidence for a novel, strongly bound acto-S1 complex carrying ADP and phosphate stabilized in the G680V mutant of Dictyostelium myosin II. *Biochemistry* **41**, 9525-9534.

Watanabe, T. M., Tanaka, H., Iwane, A. H., Maki-Yonekura, S., Homma, K., Inoue, A., Ikebe, R., Yanagida, T. and Ikebe, M. (2004). A one-headed class V myosin molecule develops multiple large (approximately 32-nm) steps successively. *Proc. Natl. Acad. Sci. USA* **101**, 9630-9635.

Win, T. Z., Gachet, Y., Mulvihill, D. P., May, K. M. and Hyams, J. S. (2001). Two type V myosins with non-overlapping functions in the fission yeast Schizosaccharomyces pombe: Myo52 is concerned with growth polarity and cytokinesis, Myo51 is a component of the cytokinetic actin ring. *J. Cell Sci.* **114**, 69-79.

Wu, X. S., Tsan, G. L. and Hammer, J. A., 3rd (2005). Melanophilin and myosin Va track the microtubule plus end on EB1. *J. Cell Biol.* **171**, 201-207.